DEPARTMENT OF COMMERCE · UNITED STATES ·
Stimulating America's Progress
1913-1988

NBS TECHNICAL NOTE 1317

U.S. DEPARTMENT OF COMMERCE/National Bureau of Standards

The Effect of a Large Rotating Scatterer in a Rectangular Cavity

D.I. Wu
D.C. Chang

The National Bureau of Standards[1] was established by an act of Congress on March 3, 1901. The Bureau's overall goal is to strengthen and advance the nation's science and technology and facilitate their effective application for public benefit. To this end, the Bureau conducts research to assure international competitiveness and leadership of U.S. industry, science and technology. NBS work involves development and transfer of measurements, standards and related science and technology, in support of continually improving U.S. productivity, product quality and reliability, innovation and underlying science and engineering. The Bureau's technical work is performed by the National Measurement Laboratory, the National Engineering Laboratory, the Institute for Computer Sciences and Technology, and the Institute for Materials Science and Engineering.

The National Measurement Laboratory

Provides the national system of physical and chemical measurement; coordinates the system with measurement systems of other nations and furnishes essential services leading to accurate and uniform physical and chemical measurement throughout the Nation's scientific community, industry, and commerce; provides advisory and research services to other Government agencies; conducts physical and chemical research; develops, produces, and distributes Standard Reference Materials; provides calibration services; and manages the National Standard Reference Data System. The Laboratory consists of the following centers:

- Basic Standards[2]
- Radiation Research
- Chemical Physics
- Analytical Chemistry

The National Engineering Laboratory

Provides technology and technical services to the public and private sectors to address national needs and to solve national problems; conducts research in engineering and applied science in support of these efforts; builds and maintains competence in the necessary disciplines required to carry out this research and technical service; develops engineering data and measurement capabilities; provides engineering measurement traceability services; develops test methods and proposes engineering standards and code changes; develops and proposes new engineering practices; and develops and improves mechanisms to transfer results of its research to the ultimate user. The Laboratory consists of the following centers:

- Applied Mathematics
- Electronics and Electrical Engineering[2]
- Manufacturing Engineering
- Building Technology
- Fire Research
- Chemical Engineering[3]

The Institute for Computer Sciences and Technology

Conducts research and provides scientific and technical services to aid Federal agencies in the selection, acquisition, application, and use of computer technology to improve effectiveness and economy in Government operations in accordance with Public Law 89-306 (40 U.S.C. 759), relevant Executive Orders, and other directives; carries out this mission by managing the Federal Information Processing Standards Program, developing Federal ADP standards guidelines, and managing Federal participation in ADP voluntary standardization activities; provides scientific and technological advisory services and assistance to Federal agencies; and provides the technical foundation for computer-related policies of the Federal Government. The Institute consists of the following divisions:

- Information Systems Engineering
- Systems and Software Technology
- Computer Security
- Systems and Network Architecture
- Advanced Computer Systems

The Institute for Materials Science and Engineering

Conducts research and provides measurements, data, standards, reference materials, quantitative understanding and other technical information fundamental to the processing, structure, properties and performance of materials; addresses the scientific basis for new advanced materials technologies; plans research around cross-cutting scientific themes such as nondestructive evaluation and phase diagram development; oversees Bureau-wide technical programs in nuclear reactor radiation research and nondestructive evaluation; and broadly disseminates generic technical information resulting from its programs. The Institute consists of the following Divisions:

- Ceramics
- Fracture and Deformation[3]
- Polymers
- Metallurgy
- Reactor Radiation

[1]Headquarters and Laboratories at Gaithersburg, MD, unless otherwise noted; mailing address Gaithersburg, MD 20899.
[2]Some divisions within the center are located at Boulder, CO 80303.
[3]Located at Boulder, CO, with some elements at Gaithersburg, MD

The Effect of a Large Rotating Scatterer in a Rectangular Cavity

D.I. Wu
D.C. Chang†

Electromagnetic Fields Division
Center for Electronics and Electrical Engineering
National Engineering Laboratory
National Bureau of Standards
Boulder, Colorado 80303-3328

†University of Colorado
Boulder, Colorado 80309

U.S. DEPARTMENT OF COMMERCE, C. William Verity, Secretary

NATIONAL BUREAU OF STANDARDS, Ernest Ambler, Director

Issued March 1988

National Bureau of Standards Technical Note 1317
Natl. Bur. Stand. (U.S.), Tech Note 1317, 40 pages (Mar. 1988)
CODEN:NBTNAE

U.S. GOVERNMENT PRINTING OFFICE
WASHINGTON: 1988

FOREWORD

This report is a result of the joint efforts and collaboration between the staff of the University of Colorado at Boulder and the Electromagnetic Fields Division of the National Bureau of Standards (NBS) in establishing a theoretical basis for the mode-stirred (reverberating) chamber. This work was a part of the doctoral dissertation work undertaken by D. I. Wu. The project was sponsored by NBS under the technical supervision of Professor David C. Chang of CU and Dr. Motohisa Kanda and Dr. Mark Ma of NBS.

The goals of this project are to understand analytically the effect of a rotating scatterer or a stirrer in a large rectangular cavity and to provide analytical tools usable in the design of an effective stirrer. The focus of this report is on a large scatterer. By examining the fundamental properties associated with a perturbing body in a cavity, we investigate the key factor which governs the effectiveness of a given stirrer. This key factor, as will be described in this report, is the shifting of the frequencies of the eigenmodes.

To illustrate the effect of eigenfrequency shifting, we use the Transmission-Line-Matrix method commonly used in waveguide analysis. The simplicity inherent in this method makes it a useful tool to analyze the effectiveness of any stirrer. By examining a 2D cavity with a 1D perturbing body, we observe an interesting analogy between the action of a large stirrer and a frequency modulator.

Previous publications under the same effort include:

Tippet, J. C.; Chang, D. C. Radiation characteristics of dipoles sources located inside a rectangular coaxial transmission line. Nat. Bur. Stand. (US), NBSIR 75-829; 1976 January.

Tippet, J. C.; Chang, D. C.; Crawford, M. L. An analytical and experimental determination of the cut-off frequencies of higher-order TE modes in a TEM cell. Nat. Bur. Stand. (US), NBSIR 76-841; 1976 June.

Tippet, J. C.; Chang, D. C. Higher-order modes in rectangular coaxial line with infinitely thin inner conductor. Nat. Bur. Stand. (US), NBSIR 78-873; 1978 March.

Sreenivasiah, I.; Chang, D. C. A variational expression for the scattering matrix of a coaxial line step discontinuity and its application to an over moded coaxial TEM cell. Nat. Bur. Stand. (US), NBSIR 79-1606; 1979 May.

Tippet, J. C.; Chang, D. C. Dispersion and attenuation characteristics of modes in a TEM cell with a lossy dielectric slab. Nat. Bur. Stand. (US), NBSIR 79-1615; 1979 August.

Sreenivasiah, I.; Chang, D. C.; Ma, M. T. Characterization of electrically small radiating sources by tests inside a transmission line cell. Nat. Bur. Stand. (US), NBS Tech Note 1017; 1980 February.

Wilson, P. F.; Chang, D. C.; Ma, M. T. Excitation of a TEM cell by a vertical electric Hertizian dipole. Nat. Bur. Stand. (US), NBS Tech Note 1037; 1981 March.

Sreenivasiah, I.; Chang, D. C.; Ma, M. T. A method of determining the emission and susceptibility levels of electrically small objects using a TEM cell. Nat. Bur. Stand. (US), NBS Tech Note 1040; 1981 April.

Wilson, P. F.; Chang, D. C.; Ma, M. T. Input impedance of a probe antenna exciting a TEM cell. Nat. Bur. Stand. (US), NBS Tech Note 1054; 1982 April.

Liu, B. H.; Chang, D. C.; Ma, M. T. Eigenmodes and the composite quality factor of a reverberating chamber. Nat. Bur. Stand. (US), NBS Tech Note 1066; 1983 August.

Wu, D. I.; Chang, D. C. An investigation of a ray-mode representation of the Green's function in a rectangular cavity. Nat. Bur. Stand. (US), NBS Tech Note 1312; 1987 September.

CONTENTS

page

FOREWORD.....iii

I. Introduction.....1

II. Small Body Perturbation.....3

III. Large Body Perturbation.....4
a) TLM Method.....7
b) Numerical Examples.....10

IV. Equivalent Effect of a Stirrer.....13

V. Conclusion.....14

References.....16

The Effect of a Large Rotating Scatterer in a Rectangular Cavity

Doris I. Wu and David C. Chang*

Electromagnetic Fields Division
National Bureau of Standards
Bouder, CO 80303

In a mode-stirred chamber, the field in the cavity is perturbed with a stirrer or rotating scatterer so that the time-averaged field is constant. In this report, we investigate the key factor which governs the effectiveness of a stirrer. By examining the fundamental properties associated with a perturbing body in a cavity, we find that the key to effective field perturbation lies in shifting the eigenmode frequencies. When the perturbing body becomes large, the shifting may be large enough that the new perturbed modes no longer resemble the original unperturbed modes. In effect, as this body rotates, different perturbed modes may be excited, thus introducing randomness into the system. We illustrate this phenomenon by examining a 2D cavity with a 1D perturbing body. Using the Transmission-Line-Matrix (TLM) method, we compute the shifting of eigenfrequencies and the variation on the magnitude of the fields for different stirrer sizes. From this analysis, we draw useful insights which include an analogy between the action of a large stirrer and a frequency modulator.

Key words: cavity perturbation; eigenfrequency; frequency shifting; mode-stirred chamber; perturbed eigenmode; stirrer; TLM method.

I. Introduction

In assessing the electromagnetic compatibility of an electronic device, we often perform tests on the susceptibility of the device to external electromagnetic field in a well defined, nonrandom environment such as a TEM cell [1] or an anechoic chamber [2]. Since the operational principles of these facilities rely on a single (dominant) mode propagation, the distribution and the polarization of the fields in these environments are invariant with time. To find the worse-case interference, it is necessary

*Department of Electrical and Computer Engineering, University of Colorado, Boulder, CO 80309

to rotate the device under test in various orientations to maximize coupling. In an attempt to eliminate the need to rotate the device being tested, we seek ways to establish an environment where the field at any location is uniformly random in time. By uniformly random we imply that the magnitude of each component of the field at each point in this environment, when sampled over a period of time, can be characterized by approximately the same maximum, minimum, and average. This uniformity feature, which in effect decreases the dependence of the device under test on its orientation as well as its location in the cavity (provided that the device is not located near any one of the cavity walls), is especially beneficial in electromagnetic interference testing.

Many researchers have shown experimentally that a uniformly random environment can be created by rotating a large scatterer, or a stirrer, in a large rectangular cavity [3,4]. Such a cavity, often called a mode-stirred or a reverberating chamber, has long been used by people in the electromagnetic compatibility area. In designing a stirrer for the mode-stirred chamber, the conventional approach is a trial-and-error, experimental process. To be able to design a good stirrer, we must know the factors which govern the effectiveness of a given stirrer. By examining the effect of a rotating scatterer in a rectangular cavity, in this report, we seek the key mechanism which causes the fields in the cavity to become uniformly random. In doing so, we hope to gain insights on other alternate methods that can be used in place of a stirrer in a rectangular cavity.

The analysis of a scatterer in a rectangular cavity begins with a small stirrer, that is, a scatterer with dimensions less than, or comparable to, a wavelength. However, since the results of the small stirrer analysis has been reported elsewhere [5,6], only a brief summary will be included in this report. The focus of this report will be on the effect of a large stirrer, or a stirrer with dimensions greater than a wavelength.

II. Small Body Perturbation

To summarize some of our earlier work, we examined the rationale for starting with a small stirrer. Without a stirrer, the field in the cavity, generally referred to as the incident field, is well behaved. The spatial variation of the field in an empty cavity operating in the multi-mode frequency range can be as high as 40 dB from point to point. In order to perturb this time-invariant, nonrandom nature of the incident field, we sought to maximize the scattered field, which was the field induced by the stirrer. Since the scattered field is proportional to the current induced on the stirrer, and the induced current is maximum when the stirrer is in resonance, we chose to start with a narrow half-wave resonating plate as the stirrer (see fig. 1). In other words, the first question we posed was whether or not the resonance of the stirrer was the key mechanism behind an effective field perturbation.

The analytical methods we used to study a small stirrer included using the method of moments to examine the distribution of the current induced on a narrow resonating plate by an incident mode in a rectangular cavity. Using this knowledge to select a proper trial current, we formulated a variational expression for the scattered field. Detailed derivations of the scattered field can be found in [6]. For a given stirrer, the scattered field was then computed numerically and compared to the incident field. Our numerical computations and experimental verification led us to the conclusion that a small resonating stirrer could not produce a scattered field large enough to perturb the incident field effectively. Therefore, a small stirrer does not have the capability of producing a uniformly random field.

Since the resonance of the stirrer failed to be the key mechanism for an effective field perturbation, we continue our search by increasing the size of the stirrer.

III. Large Body Perturbation

In searching for a strong perturbation, we turn now to an electrically large stirrer. For large stirrers, conceptually, all the analytical methods and procedures we used for the small stirrer analysis are still applicable. However, when the stirrer dimensions exceed two wavelengths, numerical computations of the induced current and the fields become extremely time-consuming and complicated. Therefore, instead of following the same procedure, we pause to re-examine some of the fundamental properties associated with a perturbing body in a cavity. In particular, we seek those features that are accentuated when the size of the perturbing body becomes large. We postulate that these accentuated features might also be the governing factors behind a strong perturbation of the incident field.

Consider a new cavity as shown in figure 2 where the perturbing body is included as a part of the cavity structure. The fields in this new cavity can be expanded using a new set of orthogonally perturbed mode functions [7,8]. These perturbed mode functions differ from the unperturbed mode functions in that they satisfy the boundary conditions on the perturbing body surface as well as on the cavity walls. Corresponding to each new perturbed mode function is a new perturbed eigenmode frequency. In essence, the effect of a perturbing body inside a cavity can be reflected through a new set of shifted eigenfrequencies and mode functions. In general, the amount of the shift for each eigenfrequency depends on the size of the perturbing body. When the size of the perturbing body becomes large, the shift for each mode will also become sensitive to the location and the orientation of the body in the cavity. The implication of this fundamental feature is that as this large body rotates, the amount of frequency shift for each mode may vary continuously. Since a shift in the eigenfrequency also implies a change in the mode field distribution, this continuous frequency shifting of eigenmode may result in the excitation of different perturbed modes at different angular positions of the body when the perturbed cavity is excited at a fixed frequency. Certainly at high frequencies where mode spacing is small, this kind of phenomenon has the potential of introducing randomness into the system.

The effect of mode shifting can best be seen by examining the distribution of modes about the operating frequency for a given cavity. Figure 3a is a cross-sectional view of the mode distribution near the operating frequency k_o in the normalized frequency plane. For a cavity with a finite composite Q [9], the bandwidth, ΔF, of the cavity is finite and can be represented by a spherical shell shown in figure 3a. If we are operating in the multi-mode frequency range when this cavity is excited at k_o, all those modes that fall within this shell are the dominant constituents of the field in the cavity. Placing a foreign body inside this cavity will cause these eigenmodes to shift. For a small body, such a narrow half-wave plate, the amount of shift for each mode is very small, almost negligible. As this plate is rotated, those modes that fall within the finite bandwidth-shell remain essentially stationary, so that the same set of excited modes remains the dominant modes regardless of the position of the plate. Therefore, very little randomness is induced. If we start to increase the size of the perturbing body, the amount of the shift for each mode will start to increase. At some point, these shifts will be large enough that each mode starts to shift in and out of the band (see fig. 3b). Consequently, when the cavity is excited at k_o, different modes will be excited as this body rotates. This random excitation of the perturbed modes is what we presumed to be the key process that introduces randomness into the cavity. Therefore, we postulate that the key mechanism behind an effective stirrer lies in the shifting of eigenfrequencies.

To check on the impact of eigenfrequency shift, we consider an extreme case. The easiest way to generate eigenfrequency shifts is to change the dimension of an empty cavity by a small amount. Thus, we perform a simple numerical simulation whereby we let one of the cavity walls be the stirrer, and instead of angular rotation, a lateral movement of the stirrer is employed. For this numerical exercise, the excitation frequency is fixed at 1 GHz (λ = 0.3 m), and the dimensions of the original cavity are a = 15.23

λ, $b = 10.17\ \lambda$, $c = 9.13\ \lambda$. Starting with $b = 10.17\ \lambda$, we move the wall parallel to the x-z plane discretely in 20 uniform steps for a total distance of one wavelength. Since the dimension of the cavity changes at each stirrer position, a new set of modes with shifted frequencies is generated correspondingly. Using an $\hat{x}$-directed unit point source to excite the cavity, we can express the field in the cavity in a modal form and can compute it easily using the hybrid representation of the dyadic Green's function for a rectangular cavity [10]. Figure 4 is a plot of the resultant $E_t = [E_x^2+E_y^2+E_z^2]^{1/2}$, obtained by averaging over the 20 discrete increments of the moving wall at 22 randomly selected observation points. The incident E_t field, which is the field obtained in the original stationary cavity, is also included on the same plot. As can be seen, when the field is averaged over all possible stirrer/wall positions, the resulting averaged field, denoted by $< E_t>_{ave}$, exhibits a uniform feature.

Having identified the potential effect in the shifting of eigenfrequencies, we would like now to have a simple method that would allow us to examine the eigenfrequency shifts associated with a more realizable stirrer. The traditional approach to finding the eigenfrequencies of an arbitrarily shaped cavity is to use the method of moments. This approach is based upon an integral equation which leads to a matrix eigenvalue problem when the method of moments is applied [11]. Though it gives accurate solutions, this method requires a very long computation time, especially when many higher-order modes are needed. Another more recently developed approach to solving the eigenfrequencies of an arbitrary shape waveguide or cavity is the Transmission-Line-Matrix (TLM) method, which is a time-domain numerical method first proposed in 1971 by Johns and Beurle to analyze a waveguide of arbitrary shape [12]. Since then many authors have expanded this method to include homogeneous and inhomogeneous lossy dielectric mediums [13-16]. The two-dimensional TLM method has also been extended to three dimensions to include a cavity of arbitrary shape and medium [17,18]. The simplicity inherent in this method makes it a much more appealing and viable approach than the method of moments. Since the principles behind a 3D TLM method are similar to those for a 2D TLM method, a brief summary of the 2D TLM method for the simplest case of a homogeneous medium will be given below.

a) TLM Method

The TLM method is an iterative method where the propagation of the plane waves in a specific medium or structure is modeled by a Cartesian mesh of transmission lines with shunt connections at each node (see fig. 5). Using a lumped-element model for each shunt node section as shown in figure 6, we can establish an equivalence between the voltage and the E_z component of a TM wave in the cavity (or the H_z component of a TE wave), and the current and the H-field (or the E-field). To excite the network, an impulse source can be placed at a selected node in the TLM mesh (see fig. 7a). Since all four branches of a node have the same characteristic impedance, this impulse will be scattered and reflected equally in all directions (see fig. 7b). The reflected pulses from each node become the incident pulses of the neighboring nodes and the process is repeated iteratively. Each iteration corresponds to a unit of time (Δt) required for a pulse to travel from one node to the next. By tracking the voltage and the current at every node throughout the mesh as a function of discrete time, we can simulate the propagation of the plane wave in the discrete time mode.

For the more general case of four impulses incident on the four branches of a node, the scattering process can be obtained by superposition of the single incident case. If we let ${}_nV_1^i$, ${}_nV_2^i$, ${}_nV_3^i$, and ${}_nV_4^i$ denote the incident voltage impulses at time $t = n\Delta t$ on any junction node, then the reflected voltages at time $(n+1)\Delta t$ can be described by the following scattering matrix equation [14]:

$$
{}_{n}\begin{bmatrix} V_1 \\ V_2 \\ V_3 \\ V_4 \end{bmatrix}^{r} = \frac{1}{2} \begin{bmatrix} -1 & 1 & 1 & 1 \\ 1 & -1 & 1 & 1 \\ 1 & 1 & -1 & 1 \\ 1 & 1 & 1 & -1 \end{bmatrix} \times {}_{n}\begin{bmatrix} V_1 \\ V_2 \\ V_3 \\ V_4 \end{bmatrix}^{i} \tag{1}
$$

Since the reflected impules at a node automatically become the incident pulses on the neighboring nodes, a relationship can be established between the incident voltages at a node (x,y) and the voltages of the neighboring nodes, that is,

$$
\begin{aligned}
{}_{n+1}V_1^i(x,y) &= {}_{n+1}V_3^r(x,y-1) \\
{}_{n+1}V_2^i(x,y) &= {}_{n+1}V_4^r(x-1,y) \\
{}_{n+1}V_3^i(x,y) &= {}_{n+1}V_1^r(x,y+1) \\
{}_{n+1}V_4^i(x,y) &= {}_{n+1}V_2^r(x+1,y).
\end{aligned} \tag{2}
$$

Therefore, by initiating the magnitudes, directions, and the positions of the excitation sources at $t = 0$, we can obtain the corresponding values of voltages at any given observation node, and at any successive time intervals by iterating equations (1) and (2) at each node in the network. The output function of the TLM method is a series of discrete impulses of varying magnitudes representing the response of the system at a specified observation point as time progresses. This output function corresponds to a discrete sampling of the E-field (or the H-field), sampled in the time domain, at a specified observation point. The frequency response at any frequency range can be obtained by performing the discrete Fourier transform on the output function. For any closed structure, the frequency response represents the mode spectrum of the structure. Intrinsic eigenmodes of the structure are reflected through the distinct peaks appearing in the frequency spectrum.

Because of the simplicity inherent in this method, one of the main advantages of the TLM method is that it can be used to analyze complicated structures with little difficulty. Depending on the property of the medium or the complexity of the waveguide structure, we can assign appropriate reflection and transmission coefficients at each node in the network. For example, if we represent the electric field in space by the voltage in the transmission line network (that is, a TM wave), then the boundaries in the TLM network would be the same as those in the real structure. So a perfectly conducting boundary in space can be simulated by a reflection coefficient of -1 for the voltage impulses. For a TE wave, the voltage in the network represents the magnetic field; therefore the boundaries in the TLM network are dual to those in the real structure. For this case, a perfectly conducting boundary in space is simulated by a reflection coefficient of +1.

As with any numerical method, the TLM method is subject to various sources of errors. These sources of errors are discussed in [19]. The two major ones are the truncation error and the velocity error. The truncation error is caused by the finite time steps used to monitor the output function. When the Fourier transform is performed on a finite series to obtain the frequency response, the result is not a line spectrum but a superposition of (sinx)/x functions. The sidelobes of (sinx)/x functions may interfere with each other causing a shift in the maxima, and thus a shift in the eigenfrequency. This truncation error can be minimized by suppressing the sidelobes using a Hanning window and increasing the iteration time steps [20]. The second major error, the velocity error, stems from the assumption used in the TLM method that all fields propagate with the same velocity in all directions. Propagation velocity in the TLM mesh depends on the direction of propagation as well as frequency. Figure 8 is a plot of the dispersion relation between the normalized velocities on the matrix and the normalized frequency for different propagation directions. On this plot, V_α is the propagation velocity in the network, c_o is the speed of light in free space, and λ is the free-space wavelength. From this figure we can see that for $\Delta\ell/\lambda << 0.25$ or for modes propagating in the diagonal direction, the propagation velocity in the network can assumed to be a constant that differs from the free space velocity by a factor of $\sqrt{2}$, that is, $v_\alpha = c_o / \sqrt{2}$. Therefore, for nondiagonally propagating modes, the assumption of equal propagation velocity is valid only when the wavelength in the TLM network is large compared with the network mesh size $\Delta\ell$. To minimize velocity error, $\Delta\ell$ must be chosen appropriately. If the response over a frequency band is of interest, a common guideline for waves propagating in the axial direction is to choose $\Delta\ell/\lambda_c << 0.25$, where λ_c is the wavelength corresponding to the highest frequency of interest. For waves propagating along the diagonal direction, a less stringent requirement of $\Delta\ell/\lambda_c < 0.25$ can be used.

b) Numerical Examples

To illustrate the use of the TLM method, we consider a cavity with a perturbing body. Since our purpose is to capture the essence of effective field perturbation, we revert to a 2D cavity with a 1D perturbing body for illustrative purposes. A given mesh size has a finite margin of error associated with it. The smaller the mesh size, the smaller the margin, but the longer the computation time. To minimize error as well as computation time, our first task is to determine the largest mesh size $\Delta\ell$ we can use to assure that the frequency shift observed in the mode spectrum is indeed caused by the perturbing body and not by the finite error embedded in the TLM method.

With the cavity dimensions fixed at a = 4.424 m, b = 3.318 m and a time step of 5 per node, we conducted a preliminary test using different mesh sizes and stirrer lengths. For a given stirrer length, we vary the mesh size and compare the resulting shifted eigenfrequencies of two arbitrarily selected lower-order modes with the corresponding unperturbed eigenfrequencies. For this computation, we set the highest frequency of interest, the cutoff frequency, at 0.172 GHz. An acceptable mesh size is one whose computed shifted eigenfrequencies are outside the margin of error for that mesh size. This computation is repeated for different stirrer lengths. Figures 9 and 10 display two examples of the eigenfrequency comparison for two different mesh sizes. Figures 9a and 10a are the computed unperturbed eigenfrequencies for a mesh size of $\Delta\ell \approx 0.15\lambda_c$ and $\Delta\ell$

$\approx 0.24\lambda_c$, respectively. The shaded areas represent the margin of error for each mesh size. Figures 9b and 10b are the corresponding perturbed frequencies for a stirrer length of a/4. Comparing figure 9b with 9a, and figure 10b with 10a, we see that the shifted eigenfrequencies are clearly outside the shaded regions for both mesh sizes. Although the margin of error is smaller for the first mesh size, we choose the second mesh size as the optimal mesh size in the remaining of our analysis on higher-order modes to minimize computation time. Since the majority of the higher-order modes will be propagating in a nonaxial direction, the margin of error associated with this second mesh size is expected to be less than the error shown in figure 10.

With a mesh size of $\Delta\ell = 0.24\lambda_c$, we analyze the eigenfrequencies of the higer-order modes. The cutoff frequency is arbitrarily fixed at 0.71 GHz, and a time step of 5 per node is used. With the dimensions of the cavity fixed at a = 4.57 m, b = 3.05 m, the total number of nodes in the network is 45 × 30. The mode spectrums about 0.7 GHz are computed for the unperturbed cavity as well as the perturbed cavity. The stirrer is centered at (0.46a,0.46b). Two stirrers of different lengths are examined at a rotational increment of 10^o. The lengths of the two stirrers are $6\Delta\ell$ ($\approx 1.4\lambda$ at 0.7 GHz) and $10\Delta\ell$ ($\approx 2.4\lambda$ at 0.7 GHz), respectively. Due to the discrete nature of the mesh network, a wire stirrer of a nonhorizontal or a nonvertical orientation is approximated by a piecewise straight line. A typical output comparison is illustrated in figure 11. The mode spectrum as shown in figure 11a is a plot of the magnitude of the E_y component as a function of frequency at a fixed observation point in an unperturbed cavity. It displays six eigenmodes near 0.7 GHz. For ease of comparison, the locations of the peaks in the mode spectrum are marked distinctly along the frequency axis. Figures 11b, c, d are the magnitudes of the E_y component at the same location in the cavity with a stirrer length of $10\Delta\ell$ oriented at ϕ = 0^o, 10^o, and 20^o, respectively. The relative positions of the unit impulse source and the observation point (location 1) are depicted in figure

12. By comparing the different plots in figure 11, we detect a distinct shifting of the eigenfrequencies as a function of ϕ.

The plots for the $6\Delta\ell$ stirrer are similar to figure 11 except that frequency shifts are not observed at every 10^0 increment of ϕ. In general, frequency shifts occur approximately at a 20^0 increment of ϕ for the $6\Delta\ell$ stirrer. This leads us to our first observation that a $6\Delta\ell$ stirrer generates less randomness than a $10\Delta\ell$ stirrer. Though it has the capability of perturbing the mode spectrum, a stirrer length of $6\Delta\ell$ ($\approx 1.4\lambda$) may not be long enough to generate a spatially uniform field.

To further confirm our observation, we use the magnitude data from the TLM method. As mentioned earlier, for a given source strength and a given observation point, the TLM method generates data on the magnitude of the E-field (or the H-field) as a function of frequency. Although these data may not agree exactly with the values obtained from the Green's function approach, these data can be used for relative comparison. Observing at a fixed frequency, we can compare the variation on the magnitude of the E-field as a function of ϕ at several observation points. An ideal random environment implies that the magnitude of the E-field averaged over one rotation, as well as the maximum and the minimum magnitudes of the E-field over one rotation, is the same regardless of the observation location. Selecting two observation points randomly (see fig. 12), we observe the variations on the E-field as a function of ϕ at several fixed frequencies near 0.7 GHz. At each sample frequency, we compare the average E-field at the two observation points. Figure 13 is an example of the variations of the total E-field at the two observation points as a function of ϕ for a stirrer length of $6\Delta\ell$. Figure 14 is the same plot for the longer stirrer of $10\Delta\ell$. Also plotted on each figure is the corresponding field in the unperturbed cavity at the two observation points. Without the stirrer, the spatial deviation of the field at these two locations is approximately 18 dB. With a stirrer length of $6\Delta\ell$, we see that while this stirrer is capable of generating a large scattered field, the average E-field (over a complete cycle) still has a rather large spatial deviation of approximately 6 dB between these two locations. With a longer stirrer, there is an increase in the effectiveness of the stirrer. The deviation in the average field for the $10\Delta\ell$ stirrer is approximately 3 dB. Therefore, to have a maximum spatial deviation of 3 dB, a stirrer with a minimum length of 2.4λ is needed to produce the desired field in a 2D cavity.

IV. Equivalent Effect of a Stirrer

Using a transfer function to characterize the action of a large stirrer brings to mind an interesting observation. Consider only those excited modes near the operating frequency. As the stirrer rotates, the frequencies corresponding to these eigenmodes would be shifted to either side of the original unperturbed frequencies. At the completion of one rotation, the frequency response of the stirrer can be characterized by figure 15a, where each spectral line represents a shifted mode. Since each mode is excited at a different amplitude, the corresponding amplitude response of the stirrer in the time domain will resemble figure 15b, where the different oscillations inside the envelope correspond to the different eigenfrequencies of figure 15a. In view of the periodic nature of the stirrer, figure 15b is a periodic function. From modulation theory, figure 15a is analogous to the spectrum of a frequency-modulated signal, and figure 15b is analogous to an amplitude-modulated signal. Therefore, we conclude that the action of a large rotating scatterer in a cavity has the same effect as a signal that has been frequency and amplitude modulated. The amplitude-modulation characteristic of a plate rotating in free space is a well documented feature [21-23]. When this rotating plate is placed inside a cavity, the amplitude-modulation feature is retained, and in addition, if the plate is large compared to a wavelength, there will also be a pronounced frequency-modulation effect enhanced by the confined boundaries of the cavity. In essence, the difference between a small stirrer and a large stirrer rests in the enhancement of the frequency-modulation effect by the large stirrer. The ineffectiveness of a small stirrer implies that to create a uniformly random environment in a cavity, both amplitude- and frequency-modulation effects must be present. Therefore, in view of these observations, we postulate that the action of a large stirrer can conceptually be simulated by doing random modulation, modulating in frequency as well as in amplitude, on the input signal.

V. Conclusion

With the use of the TLM method, we have illustrated that the key factor governing the effectiveness of a given stirrer lies in the amount of eigenfrequency shift it can induce as a function of the rotational angle. The analysis on a 2D cavity showed that when a perturbing body or a stirrer is of the order of 2 wavelengths or longer in dimension, a significant shift in the eigenfrequency spectrum can be observed. As the stirrer rotates, the shifts induced by the different angular positions of the stirrer result in the excitation of different perturbed modes, thus generating randomness into the system. When the resultant fields are averaged properly, a reduction in the spatial variation can be observed.

In all of our examples, we did not address specifically the manner in which the stirrer was being rotated. This is because the question of the rotational mechanism is secondary to the issue of minimum size required for effective stirring. If a stirrer is too small, then regardless of how it is being rotated, it can never produce a spatially uniform field. On the other hand, if a stirrer is of minimum length or greater, then the manner of rotation can be used to enhance a stirrer's effectiveness. To take full advantage of a stirrer, we need only to rotate it in such a way that it does not produce any rotational symmetry. Rotational symmetry in effect reduces randomness. When a rotational pattern is repeated, no additional stirring is gained. Therefore, unless the stirrer is extremely large, an asymmetrical rotation will always be better than a symmetrical rotation in a mode-stirred chamber.

By using a transfer function to characterize the stirrer, we drew an interesting analogy between the action of a large stirrer and the effect of frequency and amplitude modulations. Conceptually, we concluded that the stirrer could be simulated by the external modulation, both in frequency as well as in amplitude, of the input signal. Whether or not this simulation can be achieved in practice will require further analysis.

References

[1] Crawford, M. L. Generation of standard EM fields using TEM transmission cells. IEEE Trans. on EMC, EMC-16: 189-195; 1974.

[2] Ma, M. T.; Kanda, M.; Crawford, M. L.; Larsen, E. B. A review of electromagnetic compatibility/interference measurement methodologies. Proc. IEEE, Vol. 73: 388-411; 1985 March.

[3] Bean, J. L.; Hall, R. A. Electromagnetic susceptibility measurements using a mode-stirred chamber. Int. Symp. on EMC: 143-150; Atlanta; 1978 June.

[4] Crawford, M. L.; and Koepke, G. H. Operational considerations of a reverberation chamber for performing electromagnetic susceptibility/ vulnerability measurements. Nat. Bur. Stand. (US), NBS Tech Note 1092; 1986 April.

[5] Wu, D. I.; Chang, D. C. The use of a narrow plate as a stirrer in a mode-stirred chamber. URSI/AP Symp.; URSI Abstract: 55; Philadelphia; 1986 June.

[6] Wu, D. I. On the effect of a rotating scatterer in an over-moded rectangular cavity. Ph.D. dissertation, Univ. of Colorado, Boulder, CO; 1987 May.

[7] Harrington, R. F. Time-harmonic electromagnetic fields. New York, NY: McGraw-Hill, 1961.

[8] Goubau, G. Electromagnetic Waveguides and Cavities. New York, NY: Pergamon Press, 1961.

[9] Liu, B. H.; Chang, D. C.; and Ma, M. T. Eigenmodes and the composite quality factor of a reverberating chamber. Nat. Bur. Stand. (US), NBS Tech Note 1066; 1983 August.

[10] Wu, D. I.; Chang, D. C. An investigation of a ray-mode representation of the Green's function in a rectangular cavity. Nat. Bur. Stand. (US), NBS Tech Note 1312; 1987 September.

[11] Spielman, B.; Harrington, R. F. Waveguides of arbitrary cross section by solution of a nonlinear integral eigenvalue equation. IEEE Trans. MTT, MTT-20: 1495-1504; 1972.

[12] Johns, P. B.; and Beurle, R. L. Numerical solution of a 2-dimensional scattering problems using a transmission-line matrix. Proc. IEE, Vol. 118: 1203-1208; 1971 September.

[13] Johns, P. B. Application of the transmission-line matrix method to homogeneous waveguides of arbitrary cross-section. Proc. IEE, Vol. 119: 1086-1091; 1972 August.

[14] Johns, P. B. The solution of inhomogeneous waveguide problems using a transmission-line matrix. IEEE Trans. MTT, MTT-22: 209-215; 1974 March.

[15] Akhtarzad, S.; and Johns, P. B. Numerical solution of lossy waveguides: T.L.M. computer program. Electrn. Lett., Vol. 10: 309-311; 1974 July.

[16] Akhtarzad, S. Analysis of lossy microwave structures and microstrip resonators by the TLM method. Ph.D. dissertation, Univ. of Nottingham, England; 1975 July.

[17] Akhtarzad, S.; and Johns, P. B. Solution of 6-component electromagnetic fields in three space dimensions and time by the T.L.M. method. Electrn. Lett., Vol. 10: 535-537; 1974 December.

[18] Akhtarzad, S.; and Johns, P. B. Three dimensional transmission-line matrix computer analysis of microstrip resonators. IEEE Trans. MTT, MTT-23: 990-997; 1975 December.

[19] Hoefer, W. J. R. The transmission-line matrix method - theory and applications. IEEE Trans. MTT, MTT-33: 882-893; 1985 October.

[20] Saguet, P.; and Pic, E. An improvement for the TLM method. Electron. Lett., Vol. 16: 247-248; 1980 March.

[21] Lahaie, I. J.; and Sengupta, D. L. Scattering of electromagnetic waves by a slowly rotating rectangular metal plate. IEEE Trans. AP, AP-27: 40-46; 1979 January.

[22] Van Bladel, J. Electromagnetic fields in the presence of rotating objects. Proc. IEEE, Vol. 64: 301-318; 1976 March.

[23] Chuang, C. W.; and Pathak, P. H.; and Huang, C. C. On wave modulation by a rotating object. IEEE Trans. AP, AP-30: 486-489; 1982 May.

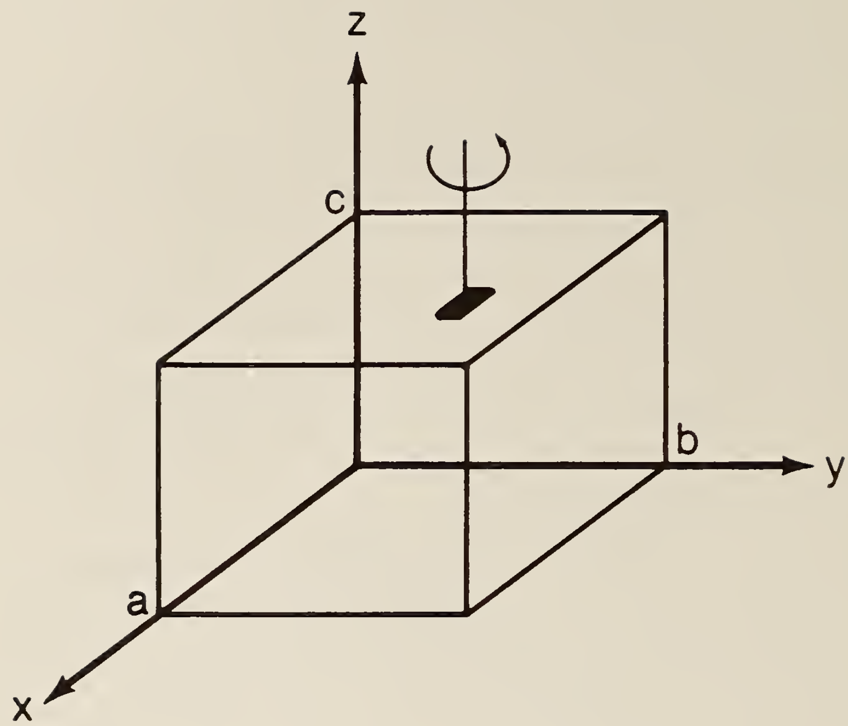

Figure 1. A rectangular cavity with a narrow plate stirrer.

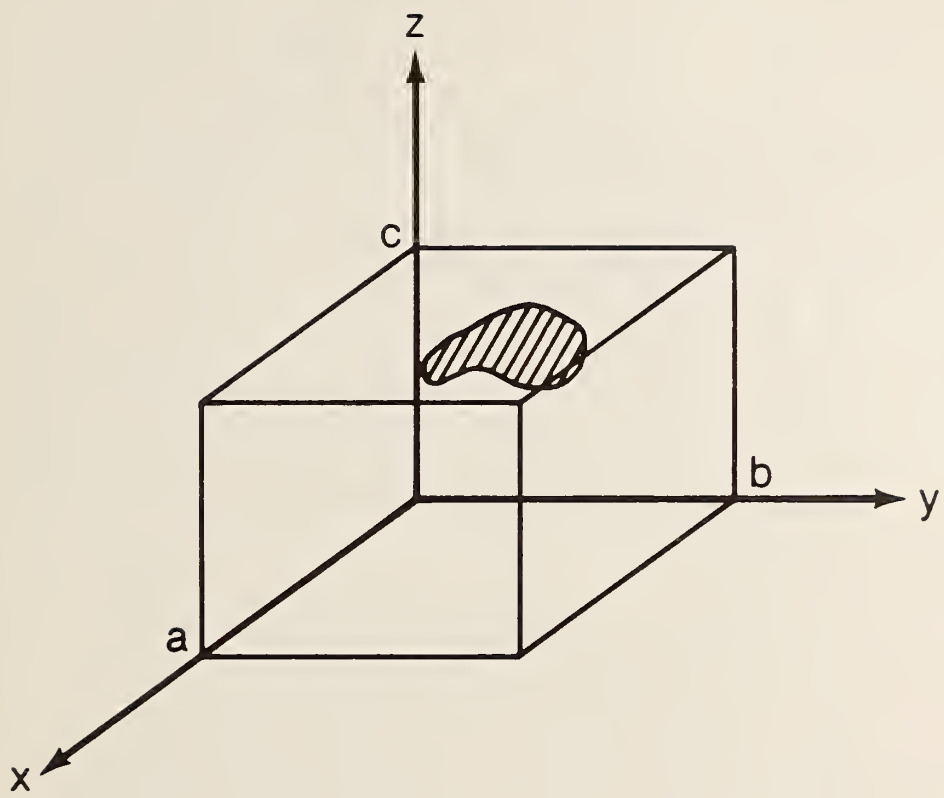

Figure 2. A rectangular cavity with a perturbing body.

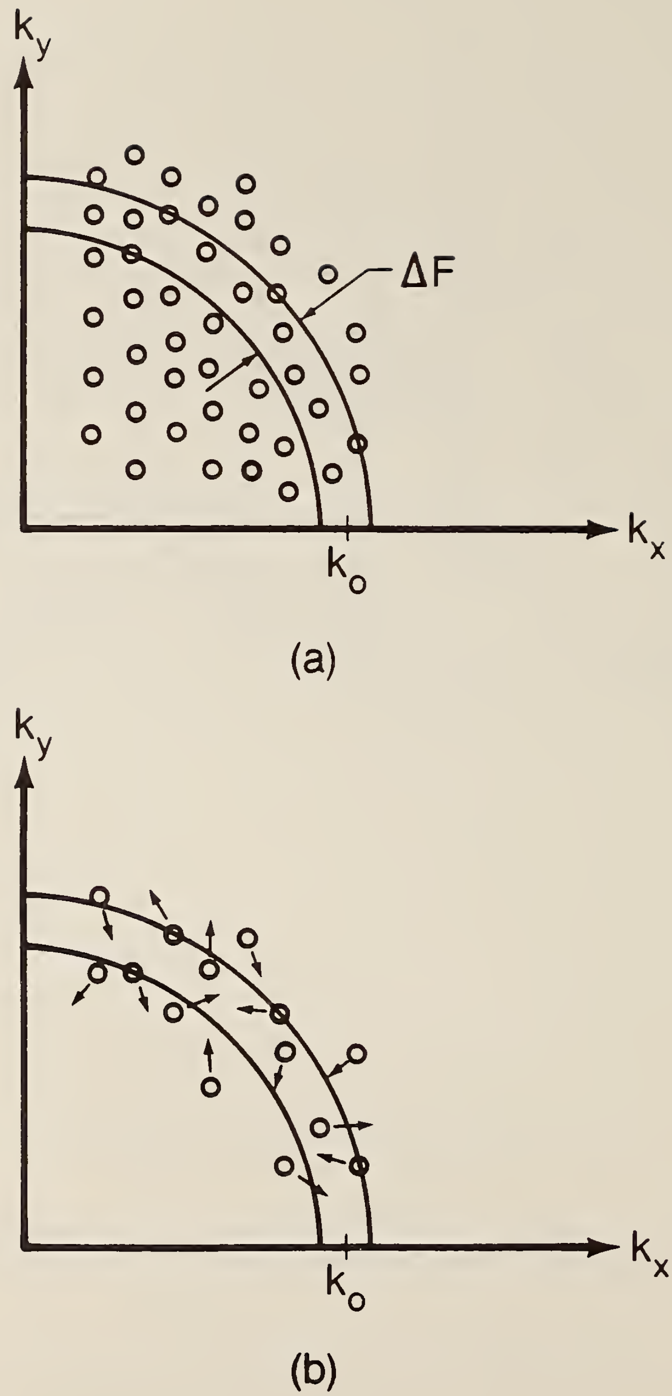

Figure 3. Mode distribution near the operating frequency k_o for a cavity with a finite bandwidth of ΔF. (a) Stationary modes. (b) Randomly shifting modes.

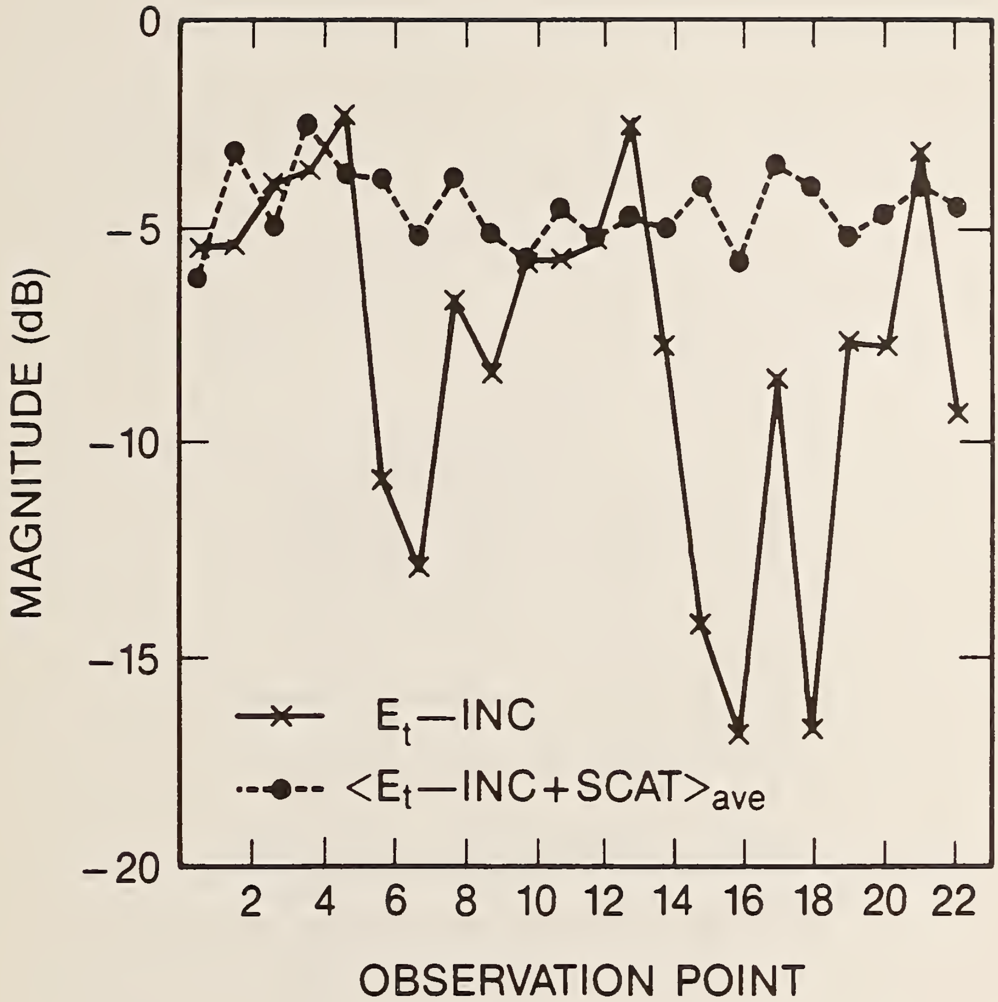

Figure 4. Comparison of the incident E_t field and the average E_t (denoted by $<E_t>_{ave}$) obtained by moving the cavity wall discretely over a small distance, for a point source excitation.

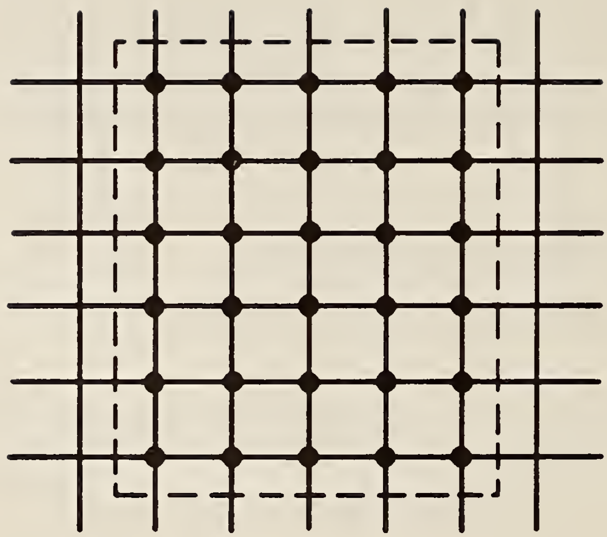

Figure 5. A Cartesian mesh of transmission lines.

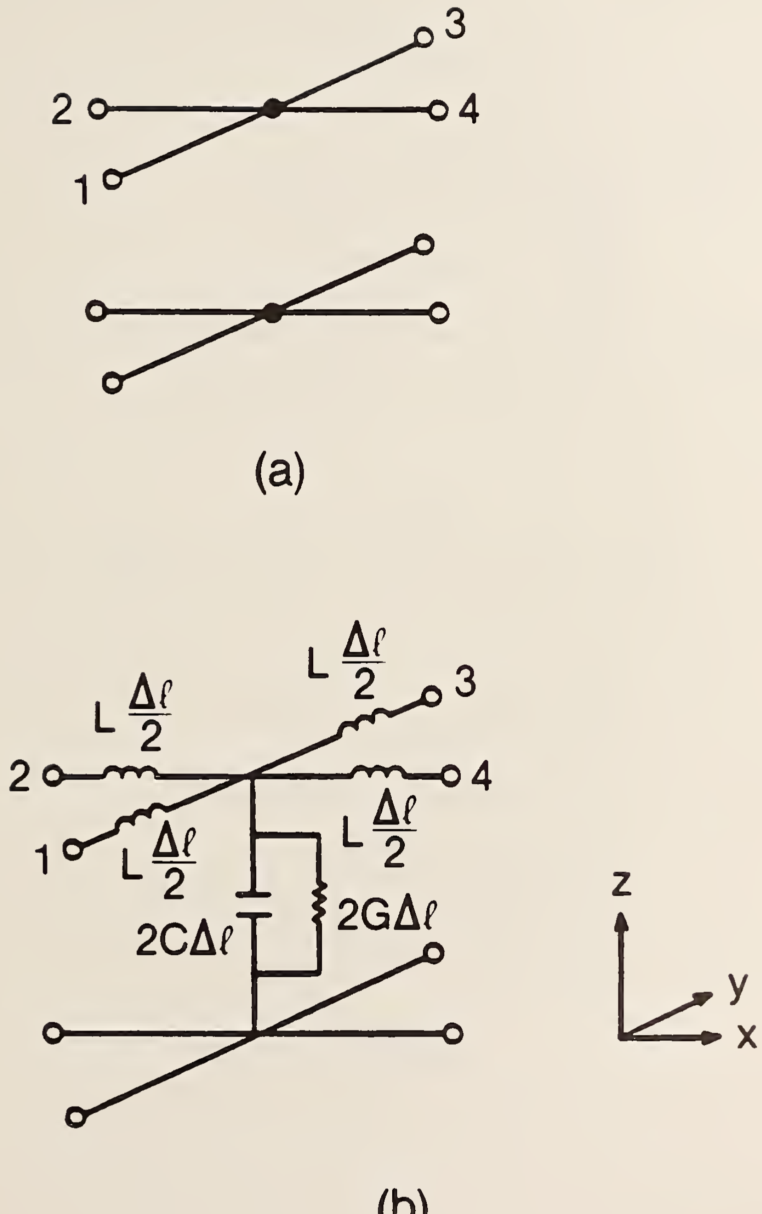

Figure 6. A shunt node section. (a) A shunt node. (b) Equivalent lumped-element model.

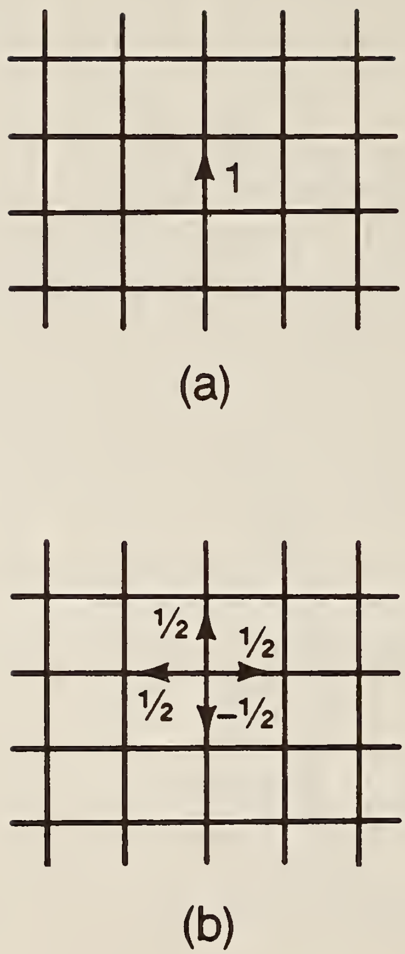

Figure 7. Scattering process in a TLM network. (a) Incident pulse. (b) Reflected pulses.

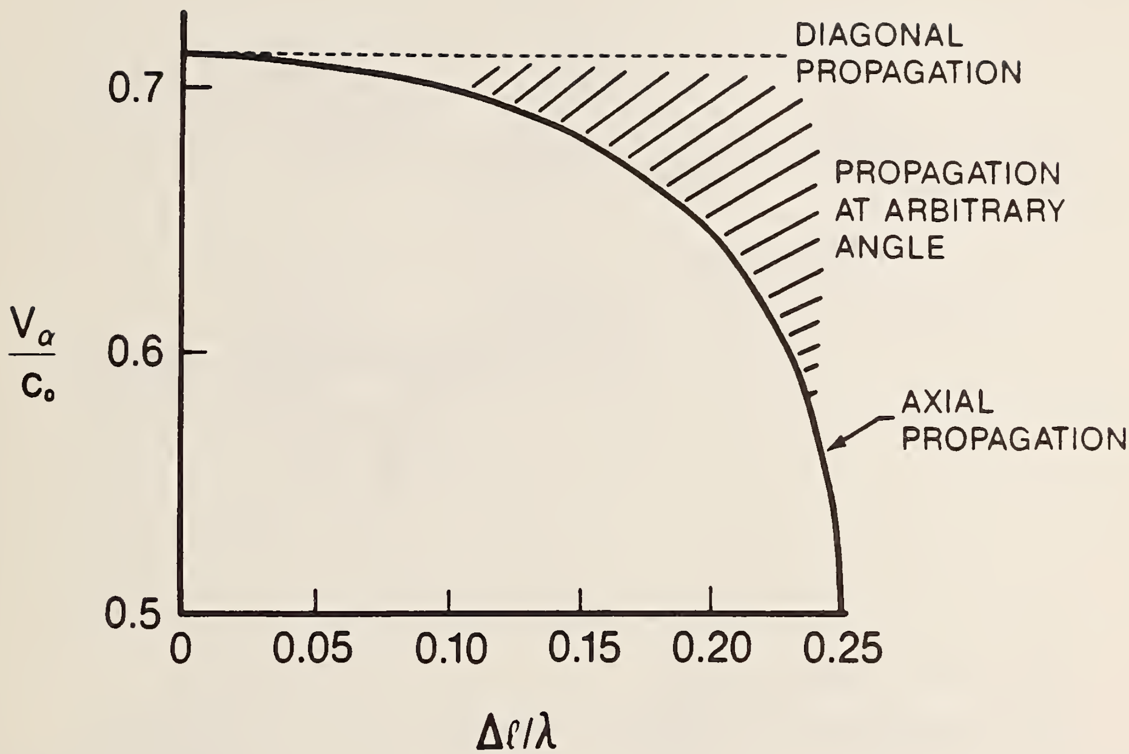

Figure 8. Dispersion of the velocity of waves in a 2D TLM network.

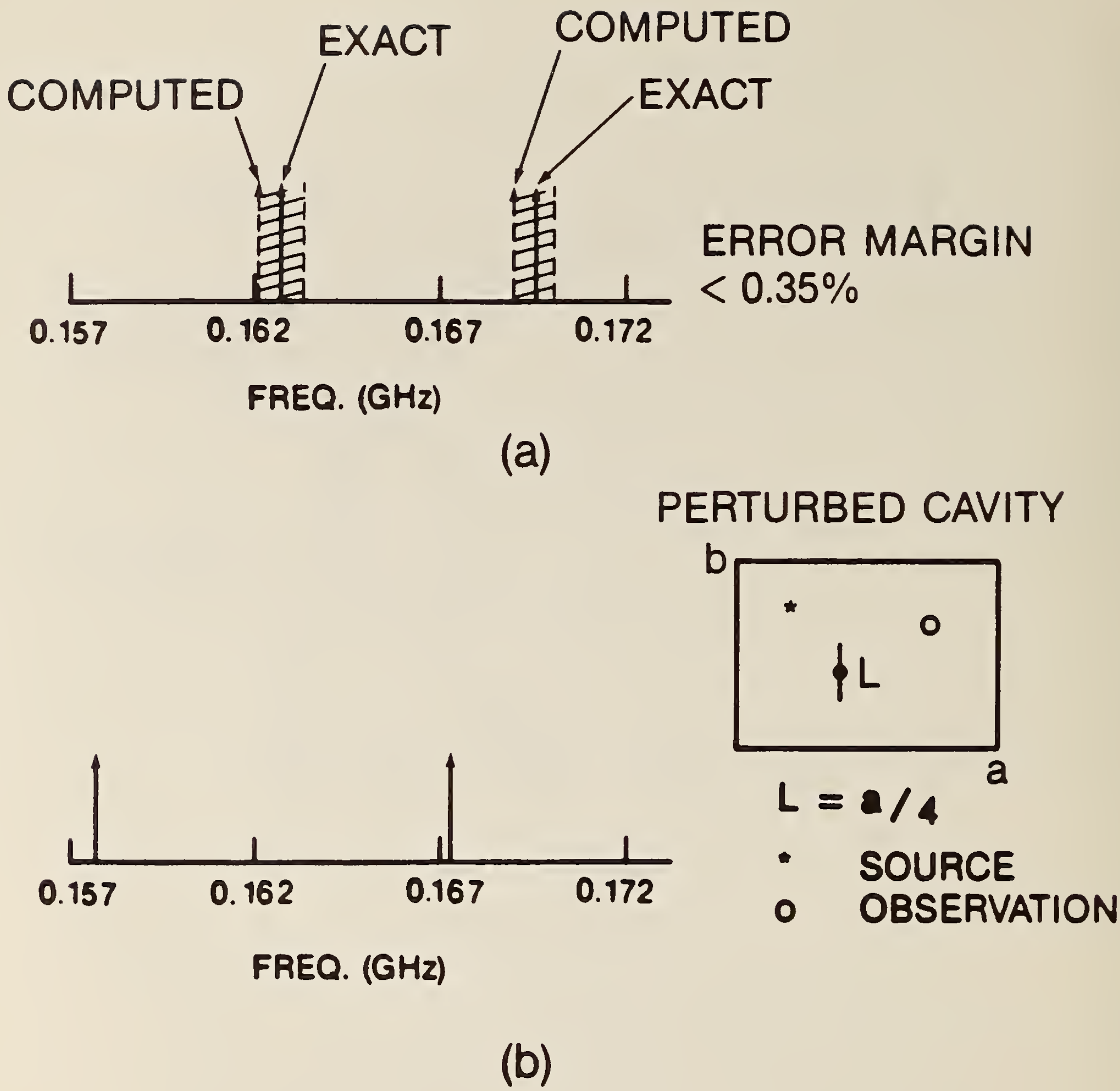

Figure 9. Computed eigenfrequencies for two lower order modes using a mesh size of $\Delta\ell \approx 0.15\lambda_c$. (a) Unperturbed eigenfrequencies, shaded area indicates the margin of error. (b) Perturbed eigenfrequencies.

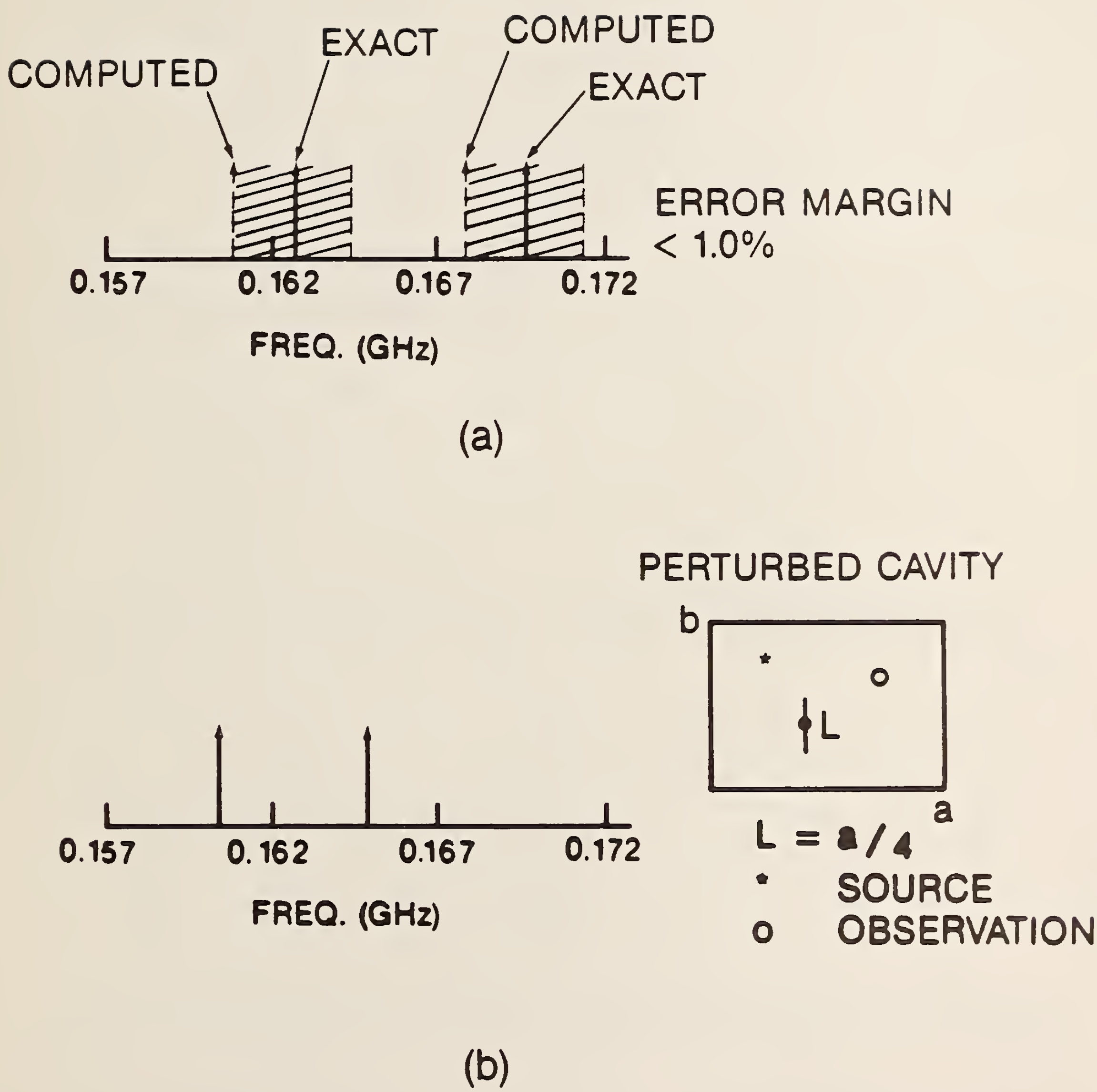

Figure 10. Computed eigenfrequencies for two lower order modes using a mesh size of $\Delta\ell \approx 0.24\lambda_c$. (a) Unperturbed eigenfrequencies. (b) Perturbed eigenfrequencies.

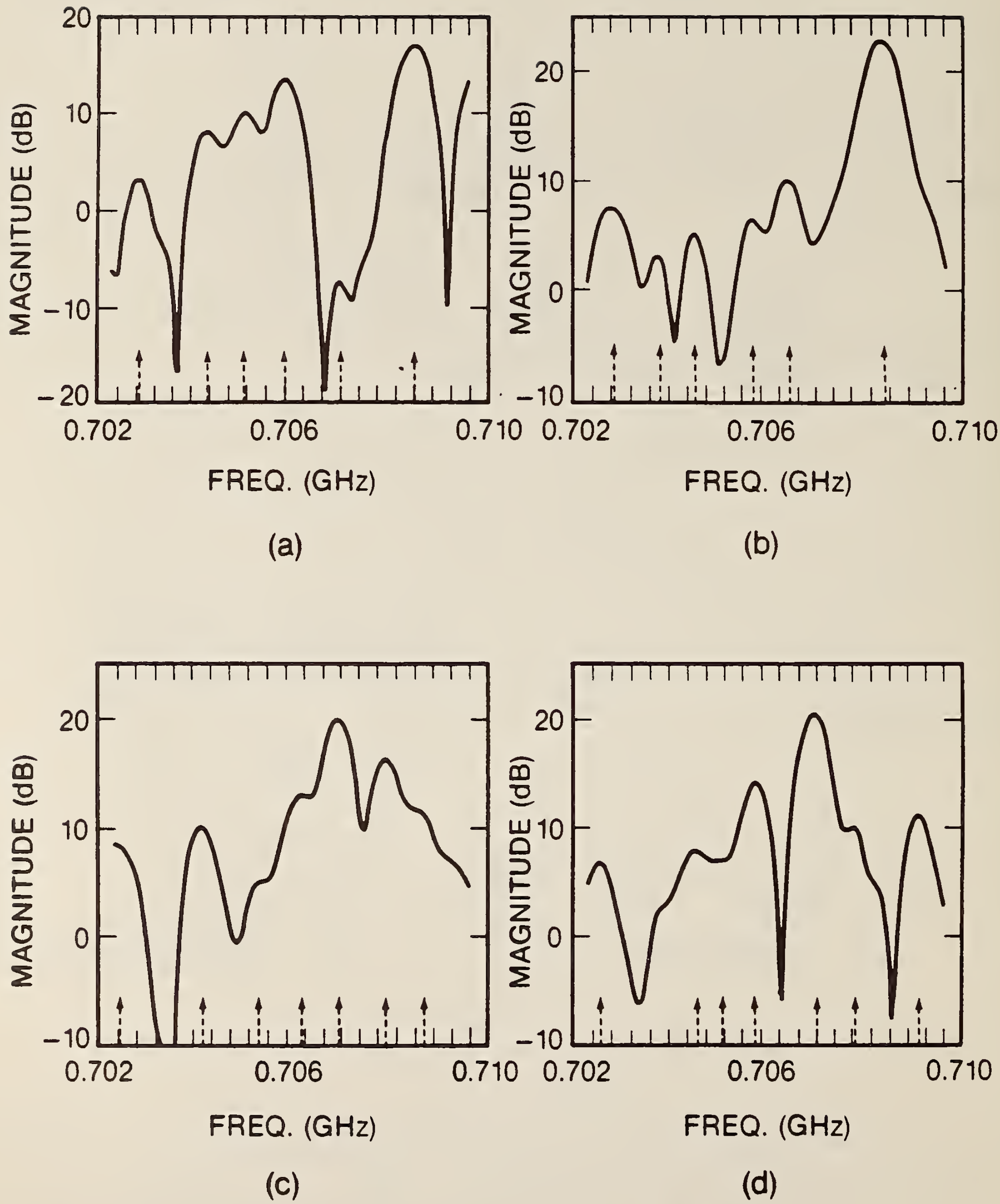

Figure 11. Mode spectrum near 0.7 GHz for an unperturbed cavity and a cavity perturbed by a $10\Delta\ell$ long stirrer of various orientations. (a) Unperturbed mode spectrum. (b) Perturbed mode spectrum for $\phi = 0^{\circ}$. (c) $\phi = 10^{\circ}$. (d) $\phi = 20^{\circ}$.

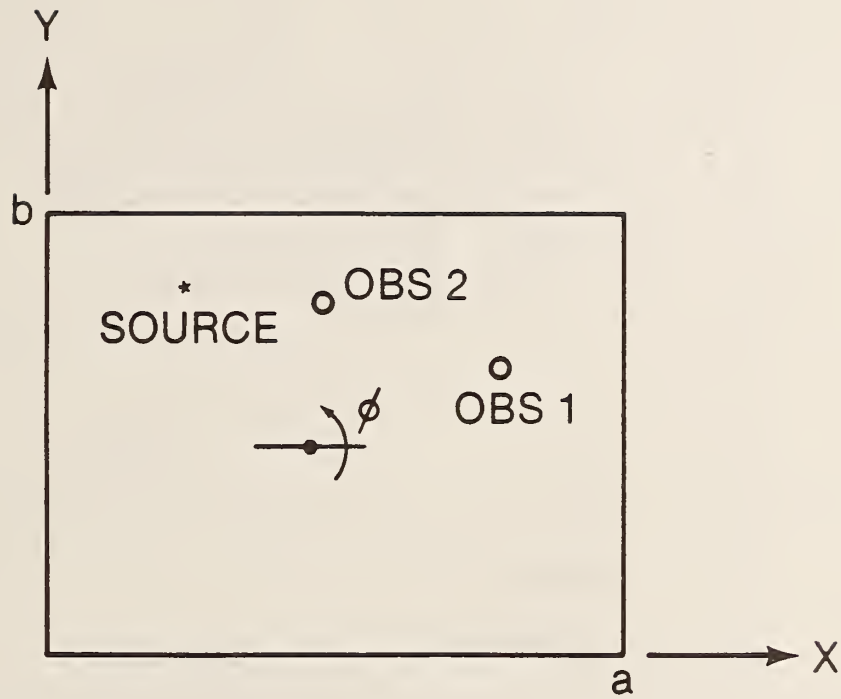

Figure 12. Relative positions of the source and the observation points in the 2D cavity.

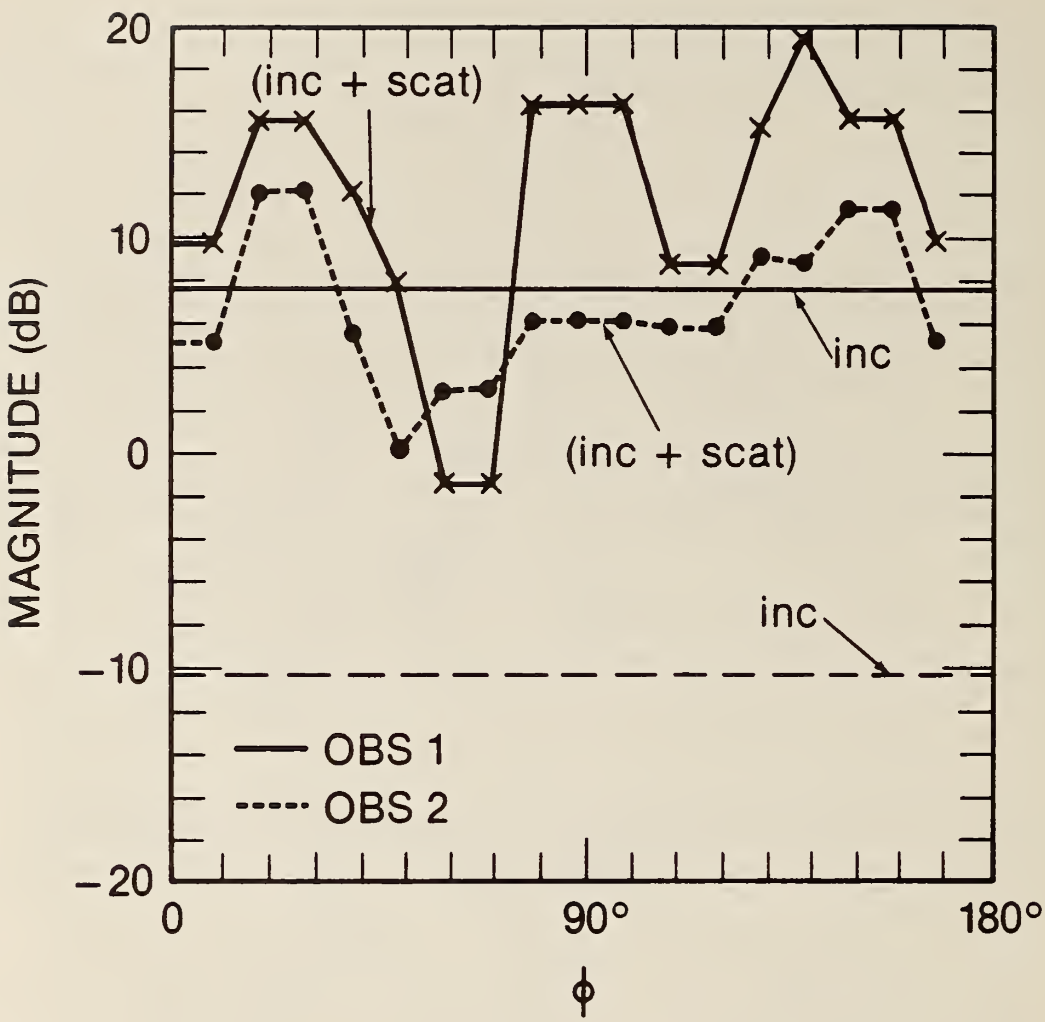

Figure 13. Variations of the total E-field at two observation points in an unperturbed cavity and a cavity perturbed by a $6\Delta\ell$ long stirrer over one rotation. Operating frequency is 0.7 GHz.

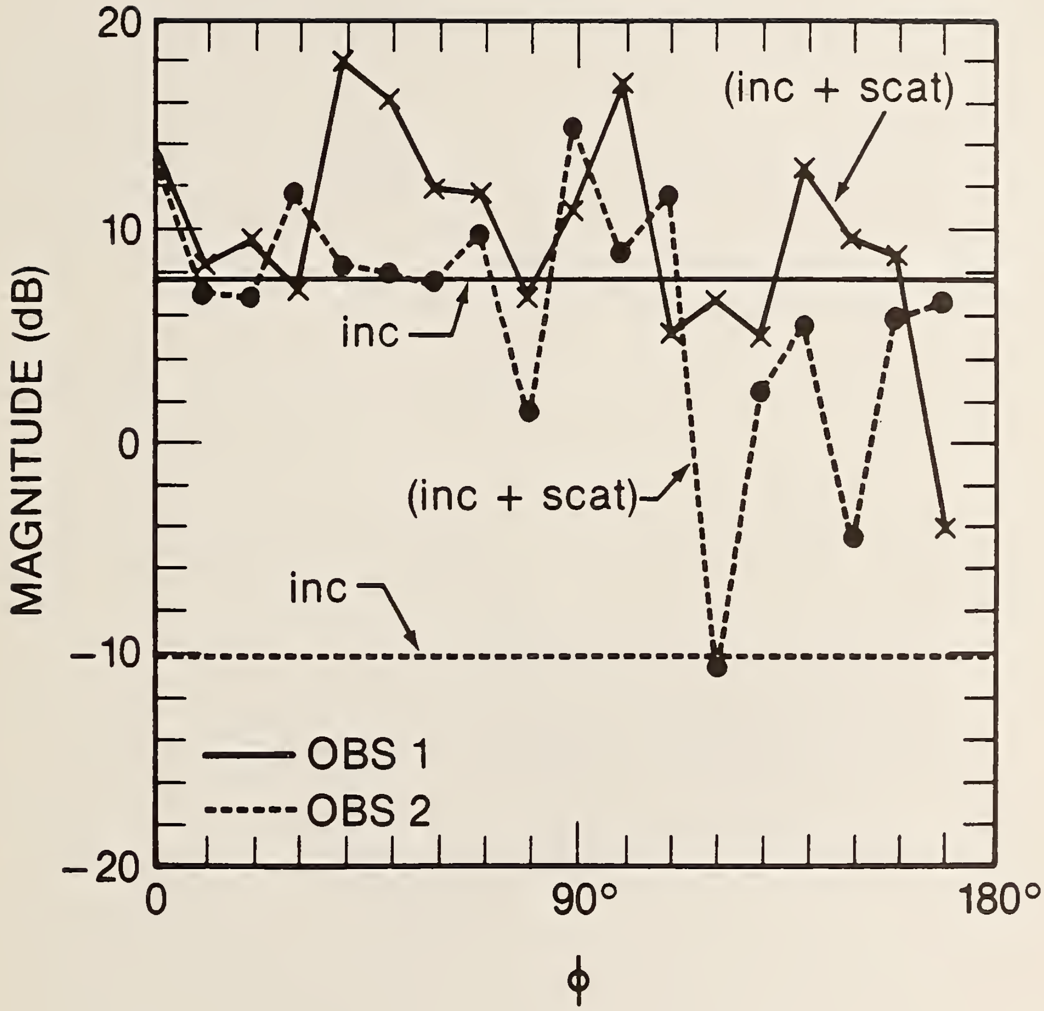

Figure 14. Variations of the total E-field at two observation points in an unperturbed cavity and a cavity perturbed by a $10\Delta\ell$ long stirrer over one rotation. Operating frequency is 0.7 GHz.

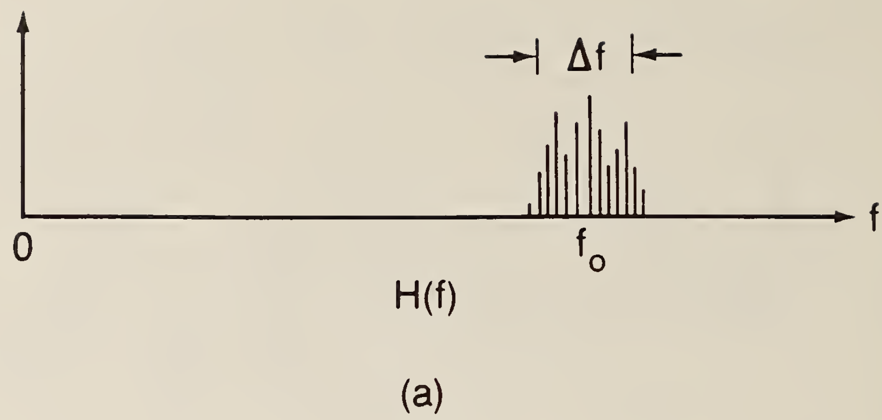

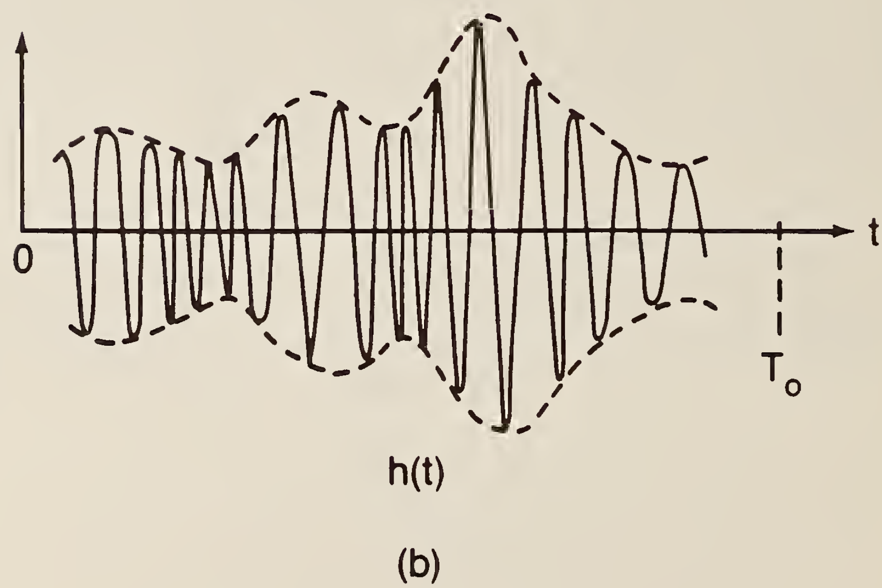

Figure 15. Transfer function for a large stirrer. (a) Frequency domain. (b) Time domain.

NBS-114A (REV. 2-80)

U.S. DEPT. OF COMM. BIBLIOGRAPHIC DATA SHEET (See instructions)	1. PUBLICATION OR REPORT NO. NBS/TN-1317	2. Performing Organ. Report No.	3. Publication Date March 1988

4. TITLE AND SUBTITLE

The effect of a large rotating scatterer in a rectangular cavity

5. AUTHOR(S)

D. I. Wu and D. C. Chang

6. PERFORMING ORGANIZATION (If joint or other than NBS, see instructions)

NATIONAL BUREAU OF STANDARDS
DEPARTMENT OF COMMERCE
WASHINGTON, D.C. 20234

7. Contract/Grant No.

8. Type of Report & Period Covered

9. SPONSORING ORGANIZATION NAME AND COMPLETE ADDRESS (Street, City, State, ZIP)

10. SUPPLEMENTARY NOTES

☐ Document describes a computer program; SF-185, FIPS Software Summary, is attached.

11. ABSTRACT (A 200-word or less factual summary of most significant information. If document includes a significant bibliography or literature survey, mention it here)

In a mode-stirred chamber, the field in the cavity is perturbed with a stirrer or rotating scatterer so that the time-averaged field is constant. In this report, we investigate the key factor which governs the effectiveness of a stirrer. By examining the fundamental properties associated with a perturbing body in a cavity, we find that the key to effective field perturbation lies in shifting the eigenmode frequencies. When the perturbing body becomes large, the shifting may be large enough that the new perturbed modes no longer resemble the original unperturbed modes. In effect, as this body rotates, different perturbed modes may be excited, thus introducing randomness into the system. We illustrate this phenomenon by examining a 2D cavity with a 1D perturbing body. Using the Transmission-Line-Matrix (TLM) method, we compute the shifting of eigenfrequencies and the variation on the magnitude of the fields for different stirrer sizes. From this analysis, we draw useful insights which include an analogy between the action of a large stirrer and a frequency modulator.

12. KEY WORDS (Six to twelve entries; alphabetical order; capitalize only proper names; and separate key words by semicolons)

cavity perturbation; eigenfrequency; frequency shifting; mode-stirred chamber; perturbed eigenmode; stirrer; TLM method.

13. AVAILABILITY

☒ Unlimited
☐ For Official Distribution. Do Not Release to NTIS
☒ Order From Superintendent of Documents, U.S. Government Printing Office, Washington, D.C. 20402.
☐ Order From National Technical Information Service (NTIS), Springfield, VA. 22161

14. NO. OF PRINTED PAGES

40

15. Price

USCOMM-DC 6043-P80

☆ U.S. GOVERNMENT PRINTING OFFICE: 1988—575-113/85,127 REGION NO. 8

NBS Technical Publications

Periodical

Journal of Research—The Journal of Research of the National Bureau of Standards reports NBS research and development in those disciplines of the physical and engineering sciences in which the Bureau is active. These include physics, chemistry, engineering, mathematics, and computer sciences. Papers cover a broad range of subjects, with major emphasis on measurement methodology and the basic technology underlying standardization. Also included from time to time are survey articles on topics closely related to the Bureau's technical and scientific programs. Issued six times a year.

Nonperiodicals

Monographs—Major contributions to the technical literature on various subjects related to the Bureau's scientific and technical activities.

Handbooks—Recommended codes of engineering and industrial practice (including safety codes) developed in cooperation with interested industries, professional organizations, and regulatory bodies.

Special Publications—Include proceedings of conferences sponsored by NBS, NBS annual reports, and other special publications appropriate to this grouping such as wall charts, pocket cards, and bibliographies.

Applied Mathematics Series—Mathematical tables, manuals, and studies of special interest to physicists, engineers, chemists, biologists, mathematicians, computer programmers, and others engaged in scientific and technical work.

National Standard Reference Data Series—Provides quantitative data on the physical and chemical properties of materials, compiled from the world's literature and critically evaluated. Developed under a worldwide program coordinated by NBS under the authority of the National Standard Data Act (Public Law 90-396).
NOTE: The Journal of Physical and Chemical Reference Data (JPCRD) is published quarterly for NBS by the American Chemical Society (ACS) and the American Institute of Physics (AIP). Subscriptions, reprints, and supplements are available from ACS, 1155 Sixteenth St., NW, Washington, DC 20056.

Building Science Series—Disseminates technical information developed at the Bureau on building materials, components, systems, and whole structures. The series presents research results, test methods, and performance criteria related to the structural and environmental functions and the durability and safety characteristics of building elements and systems.

Technical Notes—Studies or reports which are complete in themselves but restrictive in their treatment of a subject. Analogous to monographs but not so comprehensive in scope or definitive in treatment of the subject area. Often serve as a vehicle for final reports of work performed at NBS under the sponsorship of other government agencies.

Voluntary Product Standards—Developed under procedures published by the Department of Commerce in Part 10, Title 15, of the Code of Federal Regulations. The standards establish nationally recognized requirements for products, and provide all concerned interests with a basis for common understanding of the characteristics of the products. NBS administers this program as a supplement to the activities of the private sector standardizing organizations.

Consumer Information Series—Practical information, based on NBS research and experience, covering areas of interest to the consumer. Easily understandable language and illustrations provide useful background knowledge for shopping in today's technological marketplace.

Order the **above** *NBS publications from: Superintendent of Documents, Government Printing Office, Washington, DC 20402.*

Order the **following** *NBS publications—FIPS and NBSIR's—from the National Technical Information Service, Springfield, VA 22161.*

Federal Information Processing Standards Publications (FIPS PUB)—Publications in this series collectively constitute the Federal Information Processing Standards Register. The Register serves as the official source of information in the Federal Government regarding standards issued by NBS pursuant to the Federal Property and Administrative Services Act of 1949 as amended, Public Law 89-306 (79 Stat. 1127), and as implemented by Executive Order 11717 (38 FR 12315, dated May 11, 1973) and Part 6 of Title 15 CFR (Code of Federal Regulations).

NBS Interagency Reports (NBSIR)—A special series of interim or final reports on work performed by NBS for outside sponsors (both government and non-government). In general, initial distribution is handled by the sponsor; public distribution is by the National Technical Information Service, Springfield, VA 22161, in paper copy or microfiche form.

U.S. Department of Commerce
National Bureau of Standards
Gaithersburg, MD 20899

Official Business
Penalty for Private Use $300